Imex methods for thin film equations and Cahn Hilliard equations with variable mobility

Saulo Orizaga

New Mexico Tech
Department of Mathematics

University Wide Colloquium @ NMT
March 1, 2024

- Spinodal decomposition is a process in which two or more materials can separate to form different compositions.
- Phase Segregation applies to liquids and solids (polymers and metals) in different fields of science.
- Theoretical and Numerical structure for such processes

Experiment : Phase Separation

MILLER *et al.*: SPINODAL DECOMPOSITION IN Fe-Cr ALLOYS—I 3387

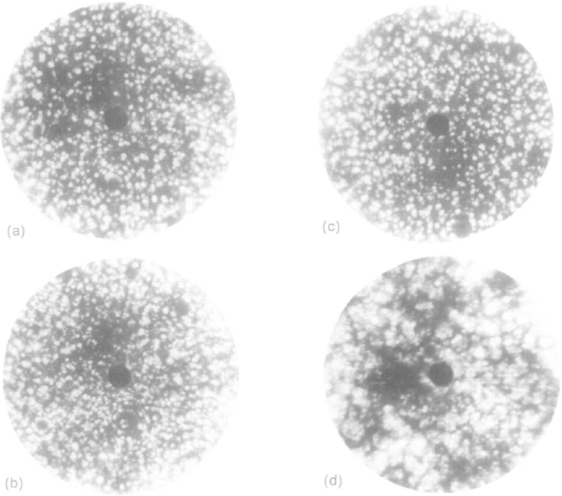

Fig. 2. Field ion micrographs from Fe 45% Cr samples aged for (a) 4, (b) 24, (c) 100 and (d) 500 h. The brightly imaging regions are Cr-enriched and the dark regions Cr-depleted.

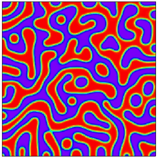

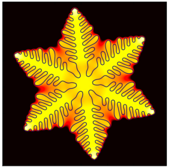

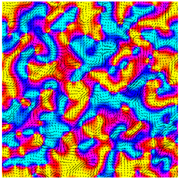

- Micro-structure evolution occurs during formation or processing of materials.
- Track evolution of interfaces, uniformity , pattern formation.
- Phases with different composition, crystalline structure, grain orientation, and structural defects.
- Spatial arrangement of the local structural features determine properties (mechanical, optical, electrical,...)
- Microstructure evolution : biology, hydrodynamics, chemical reactions,...
- Easy to add new physics : Instrument for material design

Solution structure

The solutions u evolve toward minimizers of $F(u)$ and the energy is always non-increasing. It is easy to demonstrate that any solution $u(x, t)$ in an appropriate function class will satisfy

$$\frac{d}{dt}F(u) = -\int_{\Omega} \left|\nabla \frac{\delta F}{\delta u}\right|^2 dx \leq 0.$$

Example 1: the Cahn-Hilliard equation $u_t = \Delta(-\epsilon^2 \Delta u + u^3 - u)$

The equation is the H^{-1} gradient flow of free energy

$$F(u) = \int_\Omega \frac{\epsilon^2}{2}|\nabla u|^2 + \frac{u^4}{4} - \frac{u^2}{2}\, dx.$$

Convexity splitting

$$F_+(u) = \int \frac{\epsilon^2}{2}|\nabla u|^2 + a\frac{u^2}{2} dx, \quad F_-(u) = \int \frac{u^4}{4} - [1+a]\frac{u^2}{2} dx$$

with $F_+(u)'' > 0$ and $F_-(u)'' < 0$ for $a > 2$.

$$u_t = \Delta[\delta F(u)] = \Delta[\delta F_+(u) + \delta F_-(u)]$$

$$u_t = \underbrace{\Delta[-\epsilon^2 \Delta u + au]}_{n+1-level} + \underbrace{\Delta[u^3 - (1+a)u]}_{n-level}$$

$$\frac{u_{n+1} - u_n}{h} = (-\epsilon^2 \Delta^2 + a\Delta)u_{n+1} + \Delta\Big[(u_n)^3 - (1+a)u_n\Big]. \quad \text{(CS)}$$

$$\frac{u_j^* - u_n}{h} = (-\epsilon^2 \Delta^2 + a\Delta)u_j^* + \Delta\Big[(u_{j-1}^*)^3 - (1+a)u_{j-1}^*\Big]. \quad \text{(ICS)}$$

Part III : Biharmonic Modified (BHM) Approach

$$u_t = \nabla\cdot(M(u)\nabla\delta F(u)),$$

note: if $M(u) = 1$, we get the usual CH equation $u_t = \Delta[\delta F(u)]$

$$\mathcal{F}(u) = \int_\Omega \frac{\epsilon^2}{2}|\nabla u|^2 + w(u)\, dx.$$

$$u_t = \nabla\cdot(M(u)\nabla(-\epsilon^2\Delta u + w'(u)), \qquad \text{(VMCH)}$$

Letting $\epsilon = 1$ gives

$$u_t = \nabla\cdot(M(u)\nabla[w'(u) - \Delta u]),$$

which can be written

$$u_t = \underbrace{\nabla\cdot(M(u)w''(u)\nabla u)}_{G(u)} - \nabla\cdot(M(u)\nabla\Delta u),$$

BHM approach continued

$$\frac{\partial u}{\partial t} = \underbrace{\Delta G(u) - \nabla\cdot(M(u)\nabla\Delta u)}_{F(u)},$$

where

$$G(u) = \int M(u)w''(u)\,du.$$

Introducing the splitting, the mobility coefficient function of the fourth-order operator can be written as $M(u) = M_1 + (M(u) - M_1)$ to give the form

$$\frac{\partial u}{\partial t} = \underbrace{-M_1\Delta^2 u}_{F_{\mathrm{im}}(u)} + \underbrace{\Delta G(u) - \nabla\cdot[(M(u) - M_1)\,\nabla\Delta u]}_{F_{\mathrm{ex}}(u)}$$

The main schemes

$$\frac{U_{n+1} - U_n}{h} - F_{\mathrm{im}}(U_{n+1}) = F_{\mathrm{ex}}(U_n), \qquad \text{(BHM)}$$

$$\frac{U_{(k)} - U_n}{h} - F_{\mathrm{im}}(U_{(k)}) = F_{\mathrm{ex}}(U_{(k-1)}) \quad \text{(BHM-BE}_K\text{)}$$

$$\frac{U_{(k)} - U_n}{h} - \frac{1}{2}F_{\mathrm{im}}(U_{(k)}) = \frac{1}{2}F_{\mathrm{ex}}(U_{(k-1)}) + \frac{1}{2}F(U_n) \qquad \text{(BHM-CN}_K\text{)}$$

BHM-IMEX I, 3 stage, 2nd order

$$
\begin{aligned}
U_{(0)} &= U_n, \\
U_{(1)} &= U_{(0)} + h\left(F_{\mathrm{ex}}(U_{(0)}) + F_{\mathrm{im}}(U_{(1)}) \right), \\
U_{(2)} &= \tfrac{3}{2} U_{(0)} - \frac{1}{2} U_{(1)} + h\left(\frac{1}{2} F_{\mathrm{ex}}(U_{(1)}) + \frac{1}{2} F_{\mathrm{im}}(U_{(2)}) \right), \\
U_{(3)} &= U_{(2)} + h\left(F_{\mathrm{ex}}(U_{(2)}) + F_{\mathrm{im}}(U_{(3)}) \right), \\
U_{n+1} &= U_{(3)}
\end{aligned}
$$

(Huailing Song, 2015)

BHM-IMEX II, 2 stage, 2nd order

$$
\begin{aligned}
U_{(0)} &= U_n, \\
U_{(1)} &= U_{(0)} + h\left(\gamma F_{\mathrm{ex}}(U_{(0)}) + \gamma F_{\mathrm{im}}(U_{(1)}),\right), \\
U_{(2)} &= U_{(0)} + h\left(\delta F_{\mathrm{ex}}(U_{(0)}) + (1-\delta) F_{\mathrm{ex}}(U_{(1)})\right. \\
&\qquad \left. + (1-\gamma) F_{\mathrm{im}}(U_{(1)}) + \gamma F_{\mathrm{im}}(U_{(2)})\right), \\
U_{n+1} &= U_{(2)},
\end{aligned}
$$

where $\gamma = (2-\sqrt{2})/2$ and $\delta = 1 - 1/(2\gamma)$.
(Hector D. Ceniceros 2013)

Approximate by Fourier series

$$u \approx \sum_{k_x=1}^{N} \sum_{k_y=1}^{N} \hat{u}(k,t) \exp\left[2\pi i(\omega_{k_x} x + \omega_{k_y} y)\right],$$

where $\hat{u}$ is computed via FFT.

Discrete Fourier transform is linear map $\hat{u} = \mathcal{F}u$, and Laplacian is discretized

$$\Delta u \approx \mathcal{F}^{-1}\Lambda\mathcal{F}u, \quad \Lambda\hat{u} = -(\omega_{k_x}^2 + \omega_{k_y}^2)\hat{u}$$

Operator inverses are easy by spectral mapping, e.g.

$$(I + h\Delta)^{-1}u \approx \mathcal{F}^{-1}(1 + h\Lambda)^{-1}\mathcal{F}u.$$

L_1 errors vs timestep h

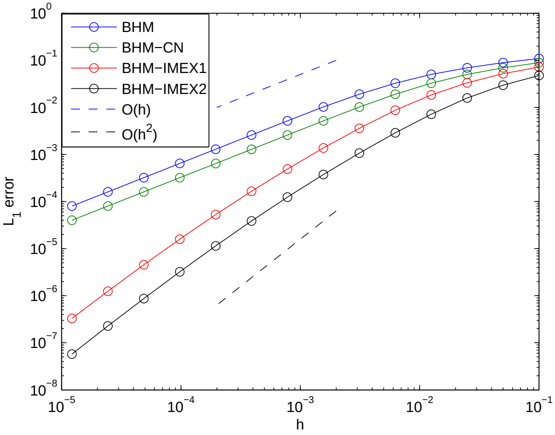

Figure: L^1-norm errors versus h of the four time-stepping schemes for the test problem using TF equation on the computational domain $[0, 12\pi]^2$ with 256×256 elements, $\epsilon = 0.1$, $t_f = 1.0$ and $M_1 = 0.32275$.

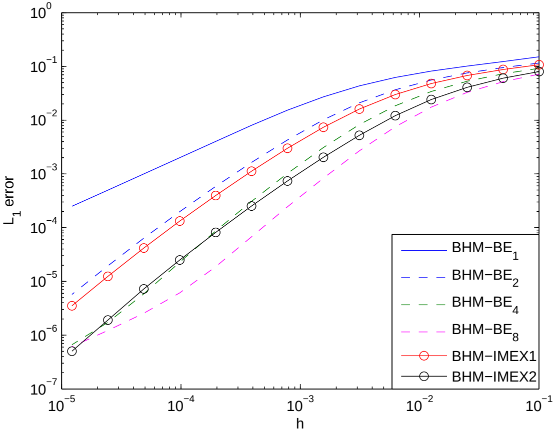
10^0
10^−1
10^−2
10^−3
10^−4
10^−5
10^−6
10^−7
L_1 error
10^−5
10^−4
10^−3
10^−2
10^−1
h
BHM−BE_1
BHM−BE_2
BHM−BE_4
BHM−BE_8
BHM−IMEX1
BHM−IMEX2

Splitting parameter M_1

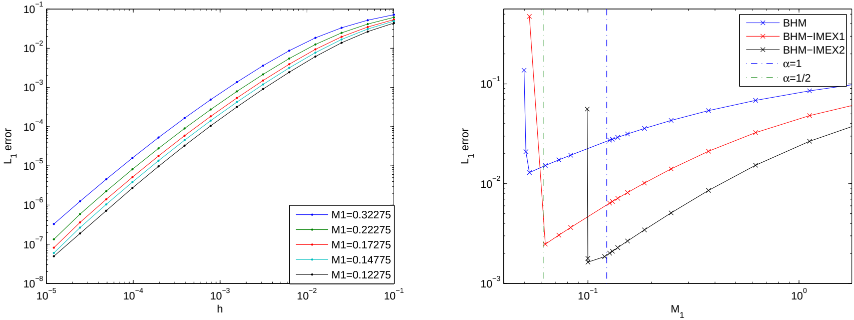

Figure: (left) BHM-IMEX1 method and various values for M_1. (right) The error for the time-stepping methods at fixed $h = 0.125$ over a range of values of M_1.

Closer look at BHM-BE$_k$

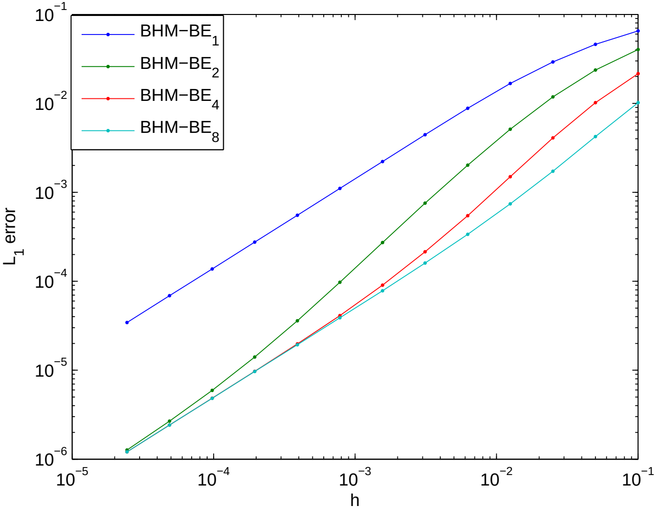

Figure: BHM-BE$_k$ using $M_1 = 0.07$.

Forced TF/CH Equation

$$u_e = 0.3 + 0.1\sin(x)\sin(y)e^{0.5t}$$

$$\frac{\partial u_e}{\partial t} = F(u_e) + \tilde{f}(x, y, t),$$

where $F(u)$ is the right hand side of the original PDE and $\tilde{f}(x, y, t) = u_{et} - F(u_e)$ is the forcing term.

Forced equation errors

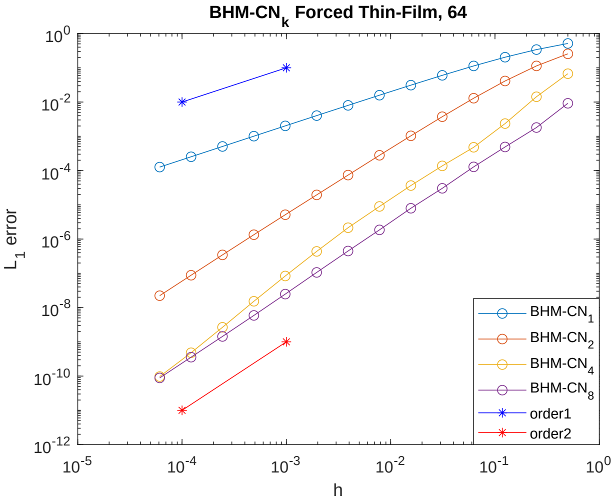

Figure: L_1 errors vs h using the forced Thin-film Equation for BHM-CN$_k$ using $M_1 = 1$.

Simulations for larger t values

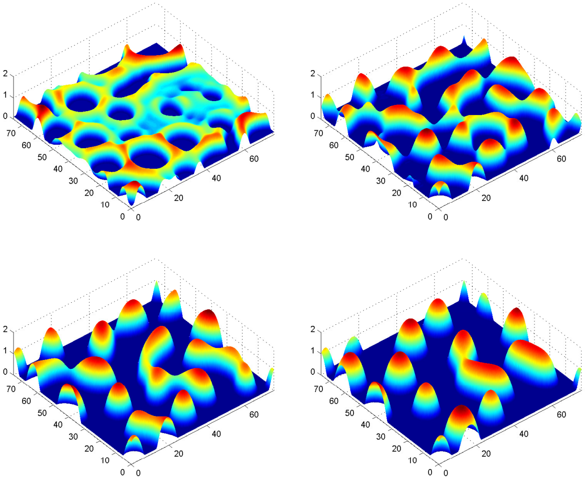

Figure: Nonlinear evolution for the solution to the thin film equation using the BHM-IMEX 2 method with $M_1 = 1$, $h = 0.1$ and $t_f = 1250$.

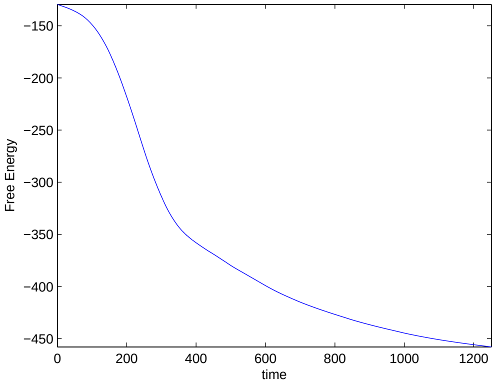

Figure: Energy evolution versus time t for the Thin film equation using BHM-IMEX 2 method with $M_1 = 5$, $h = 0.1$ and $t_f = 1250$.

Cahn-Hillliard : 3D Numerical Simulation

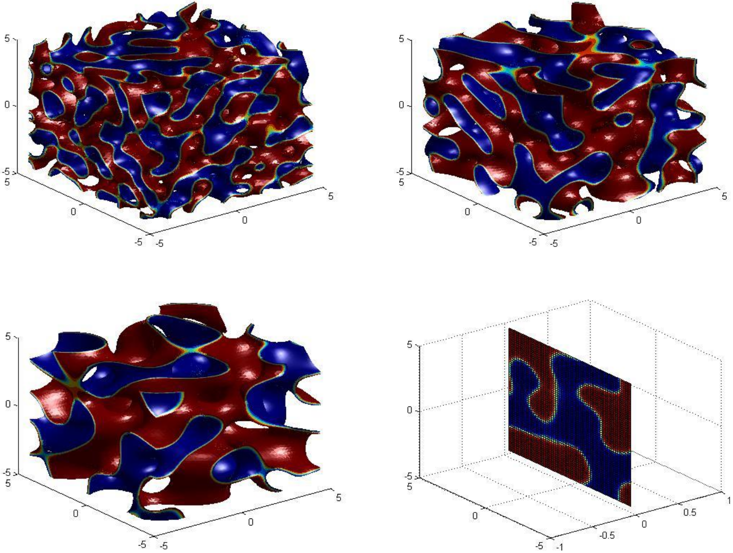

Future Work

- Cahn-Hilliard with variable mobility in 3D
- Thin-film Equation (TFE)
- Coarsening dynamics

References

1. **S. Orizaga**, K. Glasner, *Instability and reorientation of block copolymer microstructure by imposed electric fields* , Physical Review E,93, 052504 (2016)
2. Karl Glasner, **S. Orizaga**, *Improving the accuracy of convexity splitting methods for gradient flow equations*, Journal of Computational Physics 315 (2016) 52–64.
3. H. Song, Energy SSP-IMEX Runge-Kutta methods for the Cahn-Hilliard equation, J. Comput. Appl. Math., 292 (2015), pp. 576–590.
4. H. D. Ceniceros and C. J. García-Cervera. A new approach for the numerical solution of diffusion equationswith variable and degenerate mobility.J. Comput. Phys., 246:1–10, 2013.
5. A. L. Bertozzi, N. Ju, and H.-W. Lu. A biharmonic-modified forward time stepping method for fourth ordernonlinear diffusion equations.Discrete Contin. Dyn. Syst., 29(4):1367–1391, 2011.